presented at the AGARD Flight Mechanics Panel Symposium on Flight Turbulence, May 14–17, 1973, Woburn Abbey, Bedfordshire, England.

[7] Schraub, F. A. et al., "Use of Hydrogen Bubbles for Quantitative Determination of Time Dependent Velocity Fields in Low Speed Water Flows," *Transactions of the ASME, Journal of Basic Engineering*, Vol. 87, June 1965, pp. 429–444.

[8] Orloff, K. L. and Grant, G. R., "The Application of a Laser Doppler Velocimeter to Trailing Vortex Definition and Alleviation," AIAA Paper 73-680, Palm Springs, Calif., 1973.

[9] Brown, C. E., "On the Aerodynamics of Wake Vortices," *AIAA Journal*, Vol. 11, No. 4, April 1973, pp. 531–536.

[10] Govindraju, S. P. and Saffman, P. G., "Flow in a Turbulent Trailing Vortex," *The Physics of Fluids*, Vol. 14, No. 10, Oct. 1971, pp. 2074–2080.

[11] Lamb, H., *Hydrodynamics*, 6th ed., Dover, New York, 1945, pp. 591–592.

[12] Donaldson, C. duP., "Calculation of Turbulent Shear Flows for Atmospheric and Vortex Motions," *AIAA Journal*, Vol. 10, No. 1, Jan. 1972, pp. 4–12.

[13] Batchelor, G. K., "Axial Flow in Trailing Line Vortices," *Journal of Fluid Mechanics*, Vol. 20, Pt. 4, Dec. 1964, pp. 645–658.

[14] Moore, D. W. and Saffman, P. G., "Axial Flow in Laminar Trailing Vortices," *Proceedings of the Royal Society, London*, Vol. A **333**, June 1973, pp. 491–508.

[15] Owen, P. R., "The Decay of a Turbulent Trailing Vortex," *The Aeronautical Quarterly*, Vol. 21, Feb. 1970, pp. 69–78.

[16] Kuhn, G. D. and Nielsen, J. N., "Analytical Studies of Aircraft Trailing Vortices," AIAA Paper 72-42, San Diego, Calif., 1972.

[17] Squire, H. B., "The Growth of a Vortex in Turbulent Flow," *The Aeronautical Quarterly*, Vol. 16, Aug. 1965, pp. 302–306.

[18] Baldwin, B. S., Sheaffer, Y. S., and Chigier, N. A., "Prediction of Far Flowfield in Trailing Vortices," AIAA Paper 72-989, Palo Alto, Calif., 1972.

[19] Lilley, G. M., "A Note on the Decay of Aircraft Trailing Vortices," Memo 22, 1964, College of Aeronautics, Cranfield, England.

[20] Rose, R. and Dee, F. W., "Aircraft Vortex Wakes and Their Effects on Aircraft," TN Aero 2934, Dec. 1963, Royal Aircraft Establishment, Farnborough, England.

[21] Dosanjh, D. S., Gasparek, E. P., and Eskinazi, S., "Decay of a Viscous Trailing Vortex," *The Aeronautical Quarterly*, Vol. 13, May 1962, pp. 167–188.

[22] Newman, B. G., "Flow in a Viscous Trailing Vortex," *The Aeronautical Quarterly*, Vol. 10, May 1959, pp. 149–162.

[23] Templin, R. J., "Flow Characteristics in a Plane Behind the Trailing Edge of a Low Aspect Ratio Wing as Measured by a Special Pressure Probe," LM AE-58, 1954, National Aeronautical Establishment, Canada.

[24] Mabey, D. G., "The Formation and Decay of Vortices," DIC thesis, 1953, Imperial College, London.

AUGUST 1974 AIAA JOURNAL VOL. 12, NO. 8

Turbulent Boundary-Layer Flow Separation Measurements Using Holographic Interferometry

ALBERT G. HAVENER* AND ROGER J. RADLEY JR.†
Aerospace Research Laboratories, Wright-Patterson Air Force Base, Ohio

Unique experimental data are obtained from optical measurements made of a separated turbulent boundary in a supersonic, high Reynolds number flow. Holographic interferometry is used to measure density in a boundary layer that is separated from a flat surface Separation is caused by turning the boundary layer through a strong compression turn. A rational method is developed to calculate velocity distributions from the optical data with assumed conditions for the total temperature and static pressure. Also, an array of double pulse holographic interferograms is used to define qualitatively the transient behavior of a separated flow.

Introduction

HOLOGRAPHY has permitted greater flexibility in wind-tunnel testing than previously used optical techniques because the image reconstructed from the hologram contains all the information of the original density field. This means the reconstructed image can be analyzed using conventional processes. For example, shadowgrams can be obtained by focusing on different planes within the image of the density field, numerous schlieren photographs can be made simply by varying the knife edge orientation in the reconstructed image of the light source, and interferometric measurements can be made by combining the reconstructed light waves describing the flowfield with a set of reference light waves that are independent of the flowfield.

The chief motivation for this project is the successful results recently obtained from holographic interferometric measurements made of a thin, supersonic turbulent boundary layer attached to a flat surface.[1] The development of holographic wind-tunnel techniques has progressed steadily for the past few years, and the success of the attached boundary-layer investigation further demonstrates the accuracy, reliability, and capability of this flow measuring technique.[1,2]

The primary effort of this study was to use the holographic system to measure density variations in a separated boundary layer. In addition, an effort was made to calculate velocity from the density measurements. This calculation is realistic for the attached boundary layer because the total temperature and static pressure can be assumed with reasonable certainty. In the current investigation it is not obvious how to calculate velocity from density because the exact conditions for the total temperature and static pressure are unknown. Consequently, a new

Presented as Paper 73-664 at the AIAA 6th Fluid and Plasma Dynamics Conference, Palm Springs Calif., July 16–18, 1973; submitted July 10, 1973; revision received March 11, 1974. The authors acknowledge the invaluable assistance provided throughout this project by W. L. Hankey Jr. of the Hypersonic Research Laboratory, Aerospace Research Laboratories, who formulated the method for calculating velocity profiles from the optical measurements.

Index categories: Boundary Layers and Convective Heat Transfer—Turbulent; Supersonic and Hypersonic Flow.

* Captain, U.S. Air Force, Hypersonic Research Laboratory; presently Det OPNL, Sacramento Air Materiel Area, Air Force Logistics Command, McClellan Air Force Base, Calif.

† Captain, U.S. Air Force, Hypersonic Research Laboratory; presently Associate Research Engineer, United Aircraft Research Laboratories, East Hartford, Conn. Member AIAA.

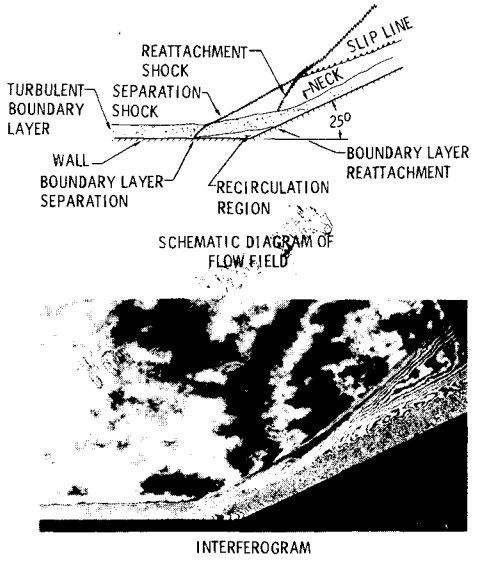

Fig. 1 Separation of the turbulent boundary layer due to a compression turn in the flow ($M_\infty = 2.96$).

method based on reasonable assumptions was developed so that velocity distributions could be calculated from the density measurements. However, it must be emphatically noted that the validity of this method depends on the validity of the assumptions, whereas the accuracy of the density data depends on the optical measurements which have been proven reliable in previous investigations.

Optical System

The optical system, described in detail in Refs. 1 and 2, is an off-axis, single-pass schlieren which is modified for holography. The light source is a Q-switched ruby laser that has a pulse width short enough (20 nsec) to record instantaneously the turbulent flow conditions or it can be double pulsed allowing high-frequency transient fluctuations to be recorded.

Two separate exposures of the subject are required to make the interferometric measurements. Usually the first exposure records the test in the no flow or undisturbed state, and the second exposure records the flow or disturbed state. These exposures can be recorded on separate holograms (dual hologram interferometry) or they can be recorded on the same hologram (double-exposure holographic interferometry). The implementation and advantages of each method are discussed completely in Refs. 1–3. Both methods are used in this investigation. Alternatively, the double pulse technique records two exposures of the flow on the same hologram. The time interval between the two exposures, however, is very accurately controlled. Intervals as small as 15 μsec and as long as 1 msec are used to determine the time scale of density fluctuations for those regions where the flow is three dimensional.

Description of Test

This investigation was conducted in the Mach 3, High Reynolds number Wind Tunnel Facility at the Aerospace Research Laboratories, Wright-Patterson Air Force Base, Ohio. The tunnel has an 8 in. × 8 in. test section, a Reynolds number range up to 10^8 per ft, and a stagnation pressure range up to 570 psi. The model is an 8 in. wide, 16 in. long flat plate that is instrumented with pressure orifices along the centerline.[4] The rear 3 in. of the model is an adjustable ramp that can be raised 30° relative to the horizontal. For the results shown herein a 25° ramp angle, a Reynolds number 9.2×10^5 per in., a stagnation pressure, and temperature of 59.6 psi and 488 R, respectively, were used.

Qualitative Results

Figure 1 shows a schematic diagram and a holographic interferogram of a turbulent boundary layer separated by a 25° compression turn. Several features of the flow are clearly recognizable in the interferogram. The recirculation region, shock structure, and boundary layer are clearly discernable, and the separation point, at which occurs a sharp rise in pressure and density, can be identified as the point where the fringe adjacent to the model surface bends sharply into the wall. The error in locating the separation point from the interferogram is no greater than the thickness of a fringe, which is approximately 0.002 in. The location of the reattachment point, however, cannot be located as accurately as the separation point because the density gradient near reattachment is small, as indicated by the wide fringe spacing along the ramp. The reattachment point can be located approximately as the point where a line extended along the reattachment shock wave intersects the wall. There is a small error in this method because the straight-line projection of the reattachment shock wave fails to account for the slight curvature in the shock wave near the model surface, which means the actual point of reattachment is further downstream of the projected point. However, the error is small because the curvature is small and also because the location determined from the wall pressure measurements[4] agrees with the location found by the linear projection of the shock wave.

An important observation is the distinctive change in the fringe pattern proceeding from the attached boundary layer through the separation region. The flow is turbulent everywhere, but the fringes in the attached boundary layer upstream of separation are typical of the parallel patterns describing laminar flow. These fringes fail to show the nonuniform, random oscillations in the turbulent flowfield because the interferogram records the total integrated change in optical pathlength that occurred over the complete 8 in. span of the model. The exposure time is very short (20 nsec) and freezes in a single instant all transient behavior so that the fringes are instantaneous, spatial averages of the density across the width of this essentially two-dimensional flowfield. Because of the spatial averaging across the two-dimensional flowfield and the small scale of the density fluctuations in the attached portion of the boundary layer, the fringes are nearly parallel. Downstream of separation, however, the waviness of the fringes strongly suggests that there are large-scale three-dimensional fluctuations.

An attempt is made to determine the time scale of the fluctuations by using double-pulse holographic interferometry in which two 20-nsec exposures of the flow are recorded on the same hologram. The time interval between the two exposures can be accurately controlled so that the fluctuations occurring on a time scale faster than a specified pulse separation can be identified by the presence of fringes (Fig. 2). When the flow is two dimensional, the spatial average of the density at any instant is constant along any given ray. Hence, a double pulsed holographic

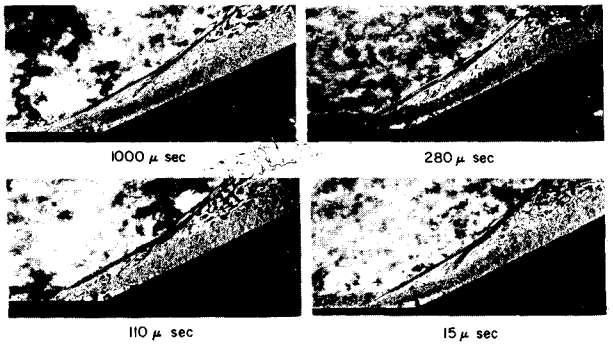

Fig. 2 Comparison of double pulsed holographic interferograms showing local disturbances and transients in the separated turbulent boundary layer.

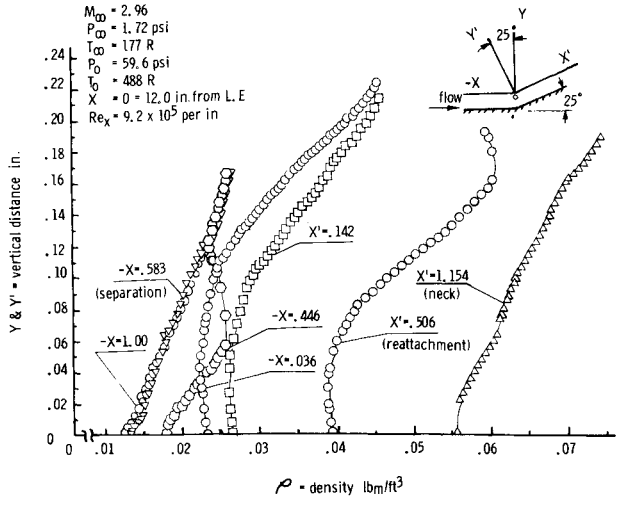

Fig. 3 Density profiles taken from the holographic interferogram shown in Fig. 1.

interferogram of this flow, regardless of the time interval between two exposures, resembles a shadowgram. Figure 2 shows that this is the case for the attached boundary layer upstream of separation. However, when the flow is three dimensional, fluctuations cause the spatial average of the density to vary with time, and a double-pulse holographic interferogram of this flow will contain fringes if the interval between exposures is longer than the time scale of the disturbance. For this particular study, the interferograms in Fig. 2 not only indicate where the flow is unsteady, but they also indicate that the time scale of the fluctuations is shorter than 15 μsec. The high frequency of the disturbances indicates that two phenomena may be causing these effects: transient oscillations, and interactions between the model and the sidewall boundary layers.

The interferograms in Fig. 2 show that the separation shock wave is stationary and does not fluctuate in time. However, transient, three-dimensional phenomena such as vortices and turbulent eddies can be generated by the strong adverse pressure gradient in the boundary layer, and these would certainly cause the spatial average of the density at each point in the flow to vary randomly with time.

The other possibility, interactions between the sidewall and model boundary layers, can be ignored for the flow upstream of separation because the flow is essentially two dimensional, and also because the thickness of the sidewall boundary layers is small compared to the 8 in. span of the model boundary layer. After separation, however, the interaction between the boundary layers is complex and difficult to determine precisely. The sidewall boundary layers may be separated or they may only be turned by the dominant compression turn of the mainstream. The exact state of the sidewall boundary layers cannot be determined from the optical data because there is no obvious way to isolate one boundary layer effect from another (other than to examine an axisymmetric model). This means the three-dimensional influences on the fringe data can only be surmised. Quantitatively, the influences are not significant because the fringes in the boundary layer maintain uniqueness and are everywhere discernable in the interferograms. Quantitatively, the three-dimensional effects can be evaluated by comparing normalized velocity profiles of the flow well downstream of reattachment with the normalized velocity profile of the upstream attached boundary layer. At a location approximately 50 boundary-layer thicknesses downstream of reattachment, the flow reaches equilibrium wherein the pressure gradients relax to zero and the total temperature is constant. Under these conditions, velocity can be calculated directly from density data, as was done in the attached boundary-layer investigation. Therefore, if three-dimensional influences have a negligible effect on the optical data, normalized velocity profiles for the fully recovered separated boundary layer should agree well with the upstream normalized profile. Unfortunately, the ramp is too short for the boundary layer to completely recover. Only ten boundary-layer thicknesses can be obtained before the ramp ends, but even in this short distance, Fig. 1 shows that the fringes are attempting to resemble the upstream configuration, which means the boundary layer is definitely approaching equilibrium. Additional comments on the calculation and comparison of normalized velocity profiles are presented in the following section.

Quantitative Results

Density is measured directly from an interferogram similar to the one shown in Fig. 1. The reference density is the density at the outer edge of the boundary layer and is calculated from the stagnation conditions and the freestream Mach number. Density for positions in the boundary layer and the separation region are calculated from the fringe shifts, and the results are presented in Fig. 3.

Unlike the velocity calculations performed for the attached boundary-layer study, those for the separated boundary layer are not straightforward. For the attached boundary layer, simplifying assumptions can be made which give accurate results. However, because of the complexity of separated boundary layers, little experimental data and essentially no accurate analytical predictions are available to serve as a basis for making assumptions necessary to compute velocity. It is obvious that velocity cannot be calculated directly from density, but density can be used with two other properties to calculate velocity. When the other two properties are unknown, however, they have to be assumed, and on this basis, the velocity calculations are performed by making reasonable assumptions for the variations in static pressure and total temperature.

The static pressure variation through the boundary layer is bounded by the edge pressure and the measured wall pressure. The pressure distribution along the wall is obtained with less than 5% error from wall orifice measurements, and to within a few percent, the pressure along the outer edge of the boundary layer is approximated by the inviscid pressure calculated from the two-dimensional oblique shock wave relationships. The correct pressure variation between the wall and edge values is given by the fact that the static pressure is constant along a Mach line. Hence, by assuming a general configuration for the shape of the Mach lines, pressure distributions can be approximated for different positions in the separated region. Figure 4 shows the variation in the wall and edge pressures. After separation, the wall pressure continually rises from the freestream static pressure while the edge pressure changes in discrete increments at two locations: separation and reattachment. After separation, the large difference between the wall and edge pressure lessens until at the corner the difference is nearly zero. The wall pressure gradient dp/dx is small in the recirculation region upstream of the corner. In this region, therefore, assuming a constant pressure through the separated boundary layer is reasonable. Elsewhere,

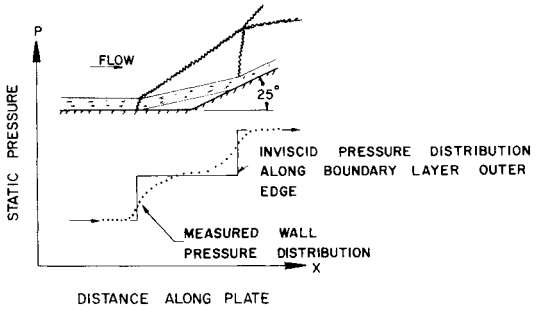

Fig. 4 Schematic diagram of wall and edge static pressure distributions for the flowfield in Fig. 1.

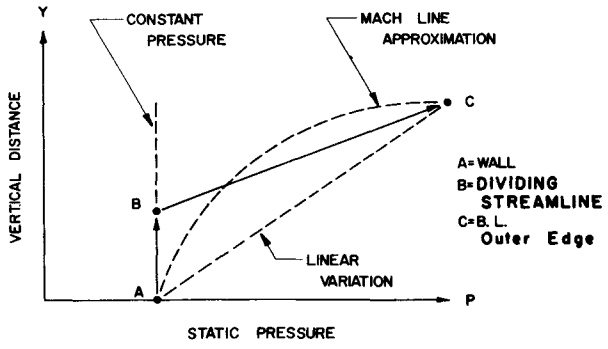

Fig. 5 Possible static pressure variations through the separated turbulent boundary layer shown in Fig. 1.

the pressure gradient along the wall is substantial, which means the constant pressure assumption is inaccurate. When dp/dx is steep, a distribution following a scheme like that shown in Fig. 5 is assumed to be reasonable. For example, the pressure is constant from the wall to the dividing streamline in the boundary layer (ideally, it is constant up to the sonic line, but the sonic line position would have to be found by iteration) after which the pressure varies linearly with distance between points B and C, the outer edge pressure. Point B is obtained from the interferogram as the point where the broad fringes in the recirculation region bend into the closely spaced fringes in the boundary layer.

Possessing knowledge of two static properties, a variation in a total property is needed. For this study, the total temperature is approximated by making a Crocco-type assumption: $T_t = C_1u + C_2$ where C_1 and C_2 are constants evaluated from the boundary conditions, $T_t = T_w$ when $u = 0$, and $T_t = T_0$ when $u = u_e$. The terms T_w, T_0 and u_e are, respectively, the wall temperature, stagnation temperature, and the velocity at the upper edge of the boundary layer. Solving for the constant C_1 and C_2, the total temperature relationship becomes

$$T_t = [(T_0 - T_w)/u_e]u + T_w \tag{1}$$

But by definition, the total temperature is

$$T_t = T + u^2/2c_p \tag{2}$$

where T is the static temperature calculated from the ideal gas law, u is the local velocity, and c_p is the specific heat at constant pressure. Combining Eqs. (1) and (2) and the ideal gas law produces

$$\frac{u^2}{2c_p} - \left(\frac{T_0 - T_w}{u_e}\right)u + \frac{p}{R\rho} - T_w = 0 \tag{3}$$

which is a quadratic equation expressing the velocity in terms of known quantities.

Two solutions are available from Eq. (3). For the flow between the wall and the maximum static temperature in the boundary layer, the negative sign is used with the discriminate, after which the positive sign is used. Equation (3) is exact for $dp/dx = dp/dy = 0$, and as shown in Fig. 4, there is only a small section in the separation region where a zero pressure gradient is approached, near the upstream side of the corner. Therefore, as a first attempt, a velocity distribution is calculated at a position 0.036 in. upstream of the corner, and the results are shown in Fig. 6. Velocity profiles for other locations are presented in Ref. 2.

Numerical difficulties arise in calculating a reverse flow velocity profile from Eq. (3). Equation (2) shows that the total temperature equals the wall temperature when the velocity is zero, and Eq. (3) shows that when the velocity is zero, the static temperature in the flow equals the wall temperature. Hence, when $u = 0$, the static and total temperature are equal, which means the profiles of these temperature distributions have to be tangent for one point in the flow. Because $T_t = T_w = T$ when $u = 0$, solutions to Eq. (3) depend greatly on determining the wall temperature. Any error in calculating T_w either causes a negative discriminant or fails to show a $u = 0$ condition for any position in the flow.

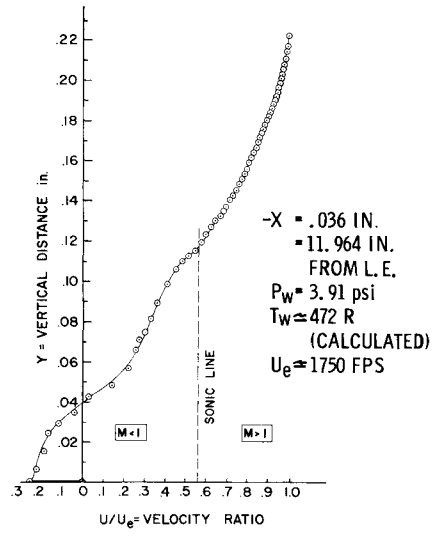

Fig. 6 Reversed flow velocity distribution calculated from the density profile at $-x = 0.036$ in.

In the most straightforward method, T_w is calculated from the ideal gas law using the measured wall pressure and the optically measured density. This value of T_w satisfies the condition $u = 0$ at the wall but it fails to give $u = 0$ for a point in the flow. Hence, there is an error in determining T_w from these measurements, which means the wall temperature must be calculated in another way. The incorrect value of T_w calculated from the measured wall pressure and density can be explained reasonably by the existence of a thin (probably on the order of 0.0005–0.001 in.) sublayer in the recirculation region. The existence of the sublayer has been shown conclusively for the attached boundary layer,[1] and also, has been reported for a separated, transonic turbulent boundary layer by other researchers.[5]

The sublayer causes a discrepancy between the density calculated from the last measurable point adjacent to the wall in the interferogram and the actual density at the wall. Across the sublayer, there is a large static temperature gradient which adjusts the flow from the stream velocity to zero at the wall.

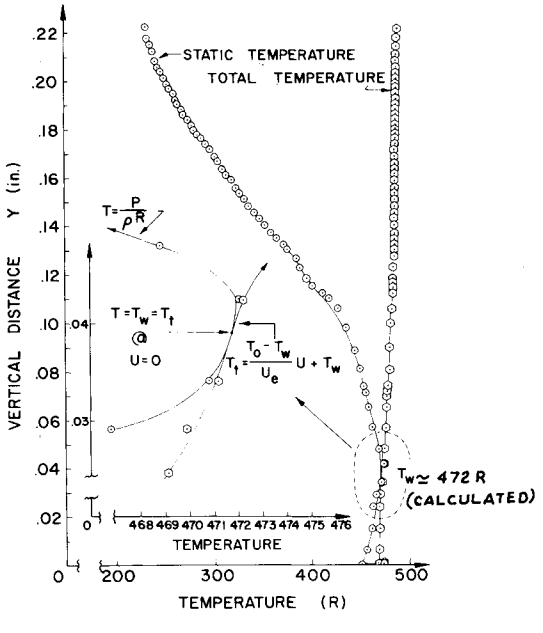

Fig. 7 Static and total temperature distributions at $-x = 0.036$ in.

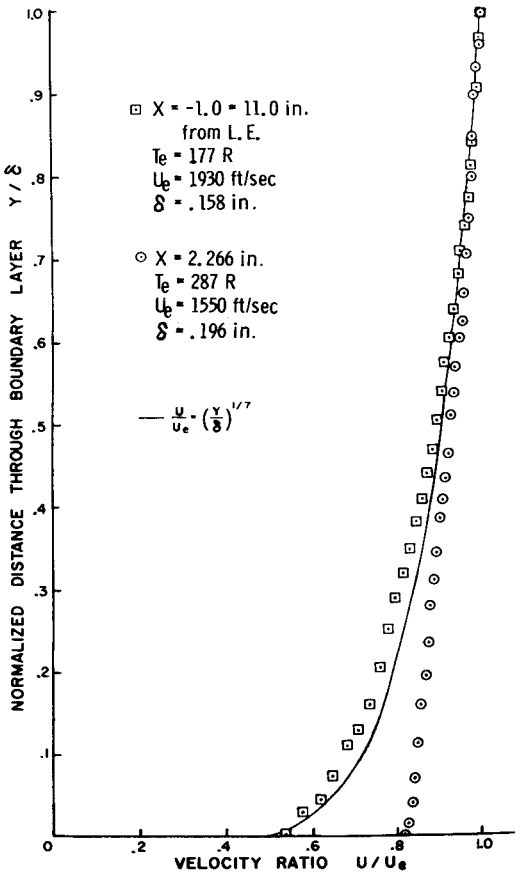

Fig. 8 Upstream and downstream attached velocity profiles based on the density data taken from Fig. 1.

The static pressure is nearly constant in the sublayer and consequently, the large temperature gradient is offset by a large density gradient. This large density gradient causes refraction which blurs the fringes at the wall. Therefore, since the wall density cannot be accurately measured, the actual wall temperature cannot be calculated directly from the ideal gas law.

The other method for determining T_w is based on the maximum value of static temperature ($T_m = p_w/R\rho_{\min}$) where the location of the minimum density $\rho_{\min}$ can be accurately determined from the optical measurements. An analytical expression for T_m is obtained by differentiating Eq. (3) with respect to u and noting that $dT/du = 0$ at $T = T_m$. This gives $u = c_p(T_0 - T_w)/u_e$ at $T = T_m$, and by substituting this relationship for u into Eq. (3) a quadratic equation is obtained and can be solved to calculate T_w from known quantities T_m, u_e, T_0. Finally, T_w is substituted back into Eq. (3) to calculate velocity distributions from the optical data, the details of which are given in Ref. 2. A profile for the position where the density gradients are nearly zero (0.036 in. upstream of the corner) is shown in Fig. 6 and the corresponding temperature distributions for T_t and T are shown in Fig. 7. It is interesting to note that for near-adiabatic walls the static temperature is very slightly less than $T_{\max}$ at $u = 0$. Additional velocity profiles are not presented here but are shown in Ref. 2 along with tabulated density data for other positions in the separation region.

Boundary-layer recoverability is evaluated by comparing normalized velocity profiles of the upstream and downstream flow conditions. Velocity profiles at $-x = 1.0$ in. and at $x = 2.266$ in. are calculated using the Crocco relationship and are compared to the $\frac{1}{7}$ power law (shown in Fig. 8). The flow properties at the outer edge of the boundary layer at $-x = 1.0$ in. are given by the freestream conditions, and those at $x' = 2.266$ in. can be calculated using the measured shock angles and simple shock theory or by using the measured wall static pressure and optically measured edge density. The first method gives $M_e = 1.89$ and the second gives $M_e = 1.97$ at $x' = 2.266$ in. This correlation shows that the fringe shift is accurate and is not distorted by three-dimensional sidewall effects. Hence, the downstream velocity profile departs from the $\frac{1}{7}$ power law because there is an insufficient distance (only ten boundary-layer thicknesses) after reattachment for the boundary layer to relax to equilibrium.

Conclusions

The objective of this project was to investigate a two-dimensional separated turbulent boundary layer using holographic interferometry. While the investigation was limited to a single case, several significant conclusions can be made. 1) The density measurements are new experimental data which can serve as a basis for future efforts, particularly analytical studies, because the interferograms are accurate. 2) While the accuracy of the velocity data relies on the validity of several important assumptions, the method used to calculate the velocity profiles revealed important mathematical requirements. Moreover, this method suggests a rational way to calculate all the fluid dynamic properties of a separated flow. 3) The inconsistencies encountered in the determination of the wall temperature very strongly suggests a thin, probably laminar, sublayer is present in the recirculation region. 4) There are definitely three-dimensional fluctuations in a two-dimensional separated boundary layer, but in this study these effects did not influence the accuracy of the optical measurements. Therefore, it is believed that the fluctuations are primarily a feature of the separation on the model rather than the result of sidewall boundary-layer interactions.

References

[1] Radley, R. J., Jr. and Havener, A. G., "The Application of Dual Hologram Interferometry to Wind-Tunnel Testing," *AIAA Journal*, Vol. 11, No. 9, Sept. 1973, pp. 1332–1333.

[2] Havener, A. G. and Radley, R. J., Jr., "Supersonic Wind Tunnel Investigations Using Pulsed Laser Holography," ARL 73-0148, Oct. 1973, Aerospace Research Lab., Wright-Patterson Air Force Base, Ohio.

[3] Havener, A. G. and Radley, R. J., Jr., "Quantitative Measurements Using Dual Hologram Interferometry," ARL 72-0085, June 1972, Aerospace Research Lab., Wright-Patterson Air Force Base, Ohio.

[4] Law, C. H., "Supersonic, Turbulent Boundary-Layer Separation Measurements at Reynolds Numbers of 10^7 to 10^8," AIAA Paper 73-665, Palm Springs, Calif., 1973.

[5] Alber, I. E., Bacon, J. W., Masson, B. S., and Collins, D. J., "An Experimental Investigation of Turbulent Transonic Viscous-Inviscid Interactions," *AIAA Journal*, Vol. 11, No. 5, May 1973, pp. 620–627.